Macromolecular Prodrugs for Controlled Delivery of Ribavirin[a]

Mille B. L. Kryger, Anton A. A. Smith, Benjamin M. Wohl, Alexander N. Zelikin*

Ribavirin (RBV)-containing polymers are synthesized based on poly(*N*-vinylpyrrolidone) and poly (acrylic acid), two polymers with extensive characterization in biomedicine. The copolymers are shown to exhibit a minor to negligible degree of association with erythrocytes, thus effectively eliminating the origin of the main side effects of RBV. The therapeutic benefit of macromolecular RBV prodrugs is illustrated by matched efficacy in suppressing production of nitric oxide by stimulated cultured macrophages as compared to pristine RBV with no associated cytotoxicity, which is in stark contrast to an RBV-based treatment which results in a significant decrease in cell viability. These results contribute to the development of antiviral polymer therapeutics and delivery of RBV in particular.

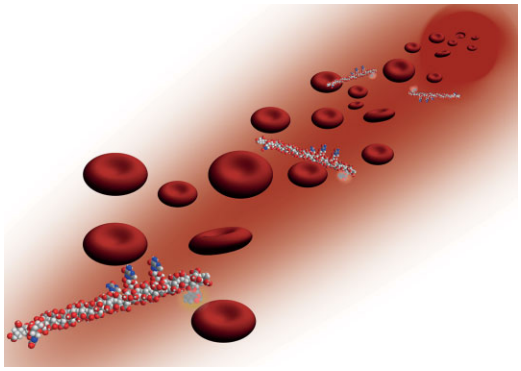

1. Introduction

Hepatitis C virus (HCV) infects millions of people worldwide. It is estimated that 3–4 million are infected each year and 130–170 million of the world population are chronically infected with HCV. Infection is often asymptomatic; nevertheless, of the chronically infected people, 60–70% progress to liver fibrosis, cirrhosis or liver cancer, and more than 350 000 people die from HCV-related liver diseases each year.[1] There are no existing vaccines to prevent the infection and the treatment based on PEGylated interferon alpha (PEG-IFN-α) and ribavirin (RBV) has a varied success rate in patients depending on the genotype of the virus. Even with the advent of direct-acting drugs against HCV, RBV has been shown to be an important factor in any treatment regime.[2]

RBV is a nucleoside analogue, first discovered in 1970,[3] with a broad antiviral effect on both DNA and RNA viruses.[4,5] Remarkably, despite decades of commercial success, the mechanism of action of RBV against HCV is still poorly understood,[6] and at least five alternative mechanisms are established, all of which require intracellular phosphorylation of RBV. In absence of clear understanding of molecular mechanism of action, origins of side effects of RBV, which include fatigue, influenza-like symptoms, gastrointestinal disturbance, neuropsychiatric symptoms and hematological abnormalities,[7] are also not well documented. This, however, is not the case for the most well documented side effect of RBV, namely accumulation in the red blood cells (RBCs). Upon cell entry, RBV is converted into its mono-, di-, and triphosphate. When this occurs within the erythrocytes, the drug is trapped within the RBCs due to lack of efficient dephosphorylation in these cells.[8] This leads to depletion of adenosine triphosphate (ATP) causing oxidative stress of the erythrocyte cell membrane and removal of the RBCs from the blood stream

M. B. L. Kryger, B. M. Wohl, Dr. A. N. Zelikin
Interdisciplinary Nanoscience Centre (iNANO), Gustav WiedsVej 14 DK-8000, Aarhus C, Denmark
A. A. A. Smith, Dr. A. N. Zelikin
Department of Chemistry, Langelandsgade 140 DK-8000, Aarhus C, Denmark
E-mail: zelikin@chem.au.dk

[a]**Supporting Information** is available from the Wiley Online Library or from the author.

DOI: 10.1002/mabi.201300244

through the reticuloendothelial system.[9,10] Accumulation of RBV in erythrocytes, which is proposed to facilitate hemolytic anaemia,[11] result in a staggering value of volume of distribution for this drug of 2000 L.[12]

In an effort to address this dose limiting side effect of RBV and facilitate delivery of this antiviral drug to the site of action, we turn to polymer therapeutics, a field of biomedical engineering which relies on polymers as intelligent carriers for therapeutic cargo.[13] Macromolecular prodrugs (MPs) offer multiple advantages for drug delivery, namely targeted delivery to the desired organs and tissues, decreased systemic distribution, subdued side effects of the drug, increased deliverable payload, etc. This concept matured from its advent into a well-developed discipline with several formulations undergoing advanced clinical trials.[13,14] Achievements of this drug delivery paradigm are sound in anticancer research; however, reports on controlled delivery of antiviral drugs using MP are few[15,16] and successes are only modest. To the best of our knowledge, there are only solitary prior examples of MP of RBV,[17–20] none of which analyzed the association of conjugated ribavirin with erythrocytes and most of which[17–19] utilized cytotoxicity of RBV as a sole readout system for intracellular drug release, that is, providing no information on therapeutic benefits of the designed polymer conjugates. The most successful implementation of MP for delivery of RBV was that by Levy et al.,[20] reporting antiviral activity of hemoglobin-conjugated RBV both in vitro and in vivo, specifically inhibition of macrophage production of pro-inflammatory cytokines and inhibition of viral replication. This report verified the promise of controlled drug delivery of ribavirin using carrier polymers and strongly suggests that broader investigation of this concept is highly warranted.

Two historically successful candidate carriers used in bioconjugation and syntheses of polymer therapeutics are poly(ethylene glycol) (PEG), and poly(hydroxypropyl methacrylamide) (HPMA). These polymers are used in most of the formulations which have progressed into clinical trials and/or reached the market.[21] Nevertheless, there is currently a growing understanding that diversity in macromolecular space is required to achieve further progress and enhanced opportunities in polymer assisted drug delivery.[22] We chose to investigate delivery of RBV using MP based on poly(*N*-vinylpyrrolidone) (PVP), and poly(acrylic acid) (PAA), two biocompatible polymers with extensive history of biomedical applications, however, scant examples of use as polymer therapeutics.

Applications of PVP in biomedicine are highly successful, go back by several decades, and include the use of this polymer as a plasma expander.[23] However, to the best of our knowledge, use of PVP in the design of MP carriers has been considered in solitary reports none of which afforded polymer samples with well controlled macromolecular characteristics. For example, radical polymerization of NVP with acrylamide-functionalized cyclodextrin (CD) monomers[24] or methacrylate derivatives of CD[25] resulted in polymers with polydispersity indexes of 1.8 and >2, respectively. These reports illustrated incompatibility of the NVP monomer with most potential comonomers for production of copolymers. This aspect minimizes opportunities in copolymerization with, for example, activated ester monomer units for bioconjugation through polymer analogous reaction.[26] Production of 'NVP-alike' monomers, i.e., derivatives of lactam structure, is a viable strategy which ensures compatibility of the monomers towards copolymerization with NVP;[27–29] nonetheless this approach is yet to be implemented in the design of MPs. Successful examples of bioconjugation with PVP include the control of polymer terminal groups via the choice of chain transfer reagents and subsequent conjugation of chain termini with proteins.[30–32] While end-on conjugation has documented utility in polymer therapeutics, including delivery of antiviral drugs,[15] this strategy has not been adopted for PVP.

Further to the most warranted, non-ionic polymers, negatively charged poly(glutamic acid) is among the most successful carriers and these polymer therapeutics progressed to advanced clinical trials. Surprisingly, other negatively charged polymers, including those used as polymer drugs,[33–36] have been largely left out of consideration as polymer carriers for MPs. Of these negatively charged polymers, PAA has been used in diverse drug delivery and related biomedical applications, specifically as mucoadhesive polymer (upon conjugation with cysteamine),[37] as polymer graft on magnetic nanoparticles for subsequent attachment of targeting ligands (folic acid),[38] in conjugation for bioseparation and stabilization of proteins,[39,40] in conjugation towards creation of combinatorial polymer-libraries,[41] as a strong adjuvant,[42,43] and extensively, as a matrix for stimuli responsive hydrogels.[44,45] However, PAA does not appear in the arsenal of tools of polymer therapeutics, specifically as a macromolecular carrier for drug molecules within injectable formulations.

Our hypothesis was that formulating RBV into MP will effectively prevent its accumulation in erythrocytes, yet once released from the polymer carrier within hepatic cells, the drug will manifest its therapeutic effect. To test this, recently, we synthesized PAA-RBV conjugate, monitored its association with erythrocytes and mammalian cells with hepatic relevance, and provided initial evaluation of RBV delivery through monitoring the production of nitric oxide by stimulated cultured macrophages.[46] In this work, we build on success of our initial study and report the results of detailed characterization of NVP- and PAA-based MPs of RBV. In particular, we describe the synthesis of a novel polymerizable form of

ribavirin, namely RBV acrylate. Tools of reversible addition/fragmentation chain transfer (RAFT) polymerization[47] are then used to obtain MPs of RBV. Resulting polymers were used in extensive in vitro tests to verify their hemocompatibility and underwent a detailed comparative analysis of polymer association with hepatic cells. Synthesized prodrugs were tested for their cytotoxicity in hepatocytes and macrophages and finally were evaluated as carriers for intracellular delivery of RBV. We strongly believe that these data contribute significantly to the development of polymer therapeutics applied for delivery of antiviral drugs.

2. Experimental Section

2.1. Materials and Methods

All materials and chemical were purchased from Sigma-Aldrich, unless stated otherwise, and used as received without further purification. Trypsin-EDTA 0.05% and Presto Blue cell viability test were purchased from Invitrogen. Ribavirin was purchased from Tokyo Chemical Industry. *Candida Antarctica lipase* 435 (Nz435 enzyme beads) was a kind gift from Novozymes. High-purity water with a resistivity of 18.2 $M\Omega\,cm^{-1}$ was obtained from a Milli-Q Direct 8 water purification system.

Flow cytometry was performed using a BD Accuri C6 flow cytometer using an excitation wavelength of 488 nm and emission detection of 530 nm. In each case at least 1 000 events were analyzed. Fluorescence and absorbance measurements were conducted using an Enspire Perkin-Elmer plate reader. Hep G2 (human liver carcinoma cell line) were cultured at 37 °C with 5% CO_2, in full cell culture medium containing minimum essential medium eagle (MEME) supplemented with fetal bovine serum (FBS, 10%), penicillin streptomycin (P/S, 1%), non-essential amino acids (NEA, 1%), and L-glutamine (2×10^{-3} M). RAW264.7 (murine monocyte macrophage cell line) was cultured at 37 °C with 5% CO_2, in full cell culture medium containing Dulbecco's modified Eagle medium (DMEM), fetal bovine serum (FBS) (10%) and P/S (1%). NMR spectra were obtained with a Varian Mercury 400 NMR spectrometer on samples dissolved in deuterated chloroform, unless stated otherwise. Chemical shifts are reported in ppm from external tetramethylsilane. MS-ESI mass spectra were obtained with a Bruker maXis Impact. Gel permeation chromatography (GPC) was performed on a system comprising a LC-20AD Shimadzu HPLC pump, a Shimadzu RID-10A refractive index detector and a DAWN HELEOS 8 LS detector. For analysing PVP polymers, Mz-Gel SDplus Linear column with 5 μm particles length of 300 mm and an internal diameter of 8 mm from MZ-Analysentechnik providing an effective molecular weight range of 1 000–1 000 000, was used with an eluent of DMF with 0.010 M LiBr at 30 °C (flow rate: 1 mL min^{-1}). For analyzing PAA polymers, HEMA-Bio Linear column with 10 μm particles, a length of 300 mm and an internal diameter of 8 mm from MZ-Analysentechnik providing an effective molecular weight range of 1 000–1 000 000, was used with an eluent was 0.1 μm filtered Milli-Q water at a flow rate of 1 mL · min^{-1} with 300 ppm sodium azide.

2.2. Syntheses

2.2.1. RBV Acrylate

Ribavirin (3 g, 12 mmol), enzyme beads (Nz435 beads, 3 g) and a few crystals of di-tert.-butylmethylphenol were suspended in 150 mL dioxane. Acetoneoxime acrylate (6.75 g, 48 mmol) was added dropwise and the reaction was stirred at 50 °C for 32 h. 500 mL MeOH was added and the mixture was filtered and reduced in vacuo followed by precipitation into diethyl ether. The precipitate is washed with 2 × 50 mL pentane to yield RBV-5-*O*-acrylate as a white powder (34%, 1.2 g, 4.1 mmol). ^{1}H NMR (DMSO-d_6): $\delta = 8.80$ (s, 1H, –N = CH–), 7.81 (s, 1H, –NH_2), 7.61 (s, 1H, –NH_2), 6.32 (dd, 1H, $J = 4$ Hz, $J = 16$ Hz, CH_2 =), 6.13 (dd, 1H, $J = 12$ Hz, $J = 16$ Hz, CH_2=), 5.90 (dd, 1H, $J = 4$ Hz, $J = 12$ Hz, $J = 4$ Hz, =CH—), 5.88 (s, 1H, N—CH—O), 5.65 (s, 1H, 3′—OH), 5.38 (s, 1H, 2′—OH), 4.25 (m, 5H, —CH_2—, —CH—O, —CH—O). ^{13}C NMR (DMSO-d_6): $\delta = 165.71$ (C=O), 160.75 (C3), 158.01 (C6), 145.90 (C5), 132.39 (CH2 =), 128.40 (=CH–), 91.87 (1′C), 81.85 (4′C), 74.59 (2′C), 70.80 (3′C), 64.48 (5′C). MS-ESI: 298.0913.

2.2.2. PVP-RBV-Fluorescein

RBV acrylate (18.7 mg, 62.7 μmol), fluorescein-*O*-acrylate (Sigma-Aldrich, 24.2 mg 62.7 μmol), phthalimidomethyl-*O*-ethyl xanthate (8.8 mg, 0.31 mmol) and azoisobutyronitrile (AIBN, 1 mg, 6.3 mmol) were dissolved in 2 mL dimethyl sulfoxide (DMSO). NVP (1.044 g, 9.4 mmol) was added and the mixture was degassed by four freeze-pump-thaw cycles. The reaction mixture was heated to 60 °C for 9 h and thereafter precipitated into diethyl ether to yield 227 mg of the copolymer. The monomer conversion was determined by ^{1}H NMR to be 35% of the NVP and full conversion of the additional monomers resulting in $\overline{M}_n$ of 12 kDa from conversion. GPC revealed $\overline{M}_n$ of 6.7 kDa and a polydispersity index (PDI) of 1.26. The RBV content was calculated from the ^{1}H NMR to be 3 mol%. ^{1}H NMR [$(CD_3)_2SO$]: $\delta = 8.80$ (bs, 1H, —N=CH—), 8.0–6.5 (broad signals, fluorescein), 7.81 (bs, 1H, –NH_2), 7.61 (bs, 1H, –NH2), 5.88 (bs, 1H, N–CH–O), 5.65 (bs, 1H, 3′—OH), 5.38 (bs, 1H, 2′—OH), 4–4.4 [bm, (m, 5H, —CH_2—, –CH–O, CH–O, –CH–)], 2.8–3.8 (broad signal, PVP polymer, 3H), 1.2–2.3 (broad signal, PVP polymer, 6H). The exact signals from the amidic protons of RBV are known from analogous polymers without fluorescein.

2.2.3. PVP-Fluorescein

Fluorescein-*O*-acrylate (3.5 mg, 9.5 μmol), phthalimidomethyl-*O*-ethyl xanthate (2.2 mg, 7.8 μmol) and AIBN (0.20 mg, 1.2 μmol) were dissolved in 0.18 mL DMSO. NVP (188 mg, 1.69 mmol) was added and the mixture was degassed by four freeze-pump-thaw cycles. The reaction mixture was heated to 70 °C for 16 h and thereafter precipitated into diethyl ether to yield 76 mg of the copolymer. The monomer conversion was determined by ^{1}H NMR to be 43% of the NVP and ≈100% for fluorescein-acrylate resulting in a $\overline{M}_n$ of 10 kDa from conversion. GPC revealed $\overline{M}_n$ of 15 kDa and a PDI of 1.7.

2.2.4. PAA-RBV-Fluorescein

A Schlenk tube was charged with cyanomethyldodecyl trithiocarbonate (12.5 mg, 0.039 mmol), AIBN (1.6 mg, 0.01 mmol), 1 equiv.

fluorescein acrylate (15.2 mg, 0.039 mmol), RBV acrylate (206 mg, 0.703 mmol), acrylic acid (AA, 1.00 g, 13.8 mmol) and 3 mL DMF. The mixture was degassed by three freeze-pump-thaw cycles and polymerized for 7.5 h at 60 °C. The conversion was determined by ^{1}H NMR to be 68%. The reaction mixture was precipitated into diethyl ether, redissolved in MeOH, and precipitated into diethyl ether again to yield 670 mg of the polymer. Resulting polymer had $\overline{M}_n$ 17 kDa as calculated from conversion, $\overline{M}_n$ 27 kDa and PDI of 1.16 from gel permeation chromatography (GPC) analysis and RBV acrylate content of 4.5 mol% determined by NMR. ^{1}H NMR [$(CD_3)_2SO$]: $\delta = 12.25$ (bs, 1H, COOH), 8.80 (bs, 1H, –N = CH–), 7.81 (bs, 1H, –NH2), 7.61 (bs, 1H, –NH2), 5.88 (bs, 1H, N–CH–O), 4–4.4 [bm, (m, 5H, –CH2—, –CH–O, –CH–O, –CH–)], 2.0–2.3 (bs, 1H, PAA polymer backbone), 1.25–1.75 (broad signal, 2H, PAA polymer backbone). RBV content was calculated from the ratio of the $\delta = 8.80$ RBV signal to the polymer backbone.

2.2.5. PAA-Fluorescein

A Schlenk tube was charged with cyanomethyldodecyl trithiocarbonate (13.2 mg, 0.042 mmol), AIBN (0.7 mg, 0.004 mmol), 1 equiv. fluorescein acrylate (16.1 mg, 0.042 mmol), AA (1.00 g, 13.8 mmol) and 1 mL DMF. The mixture was degassed by three freeze-pump-thaw cycles and polymerized for 3 h at 65 °C. The conversion was determined by NMR to be 63%. The reaction mixture was precipitated into diethyl ether, redissolved in MeOH, and precipitated into diethyl ether again to yield 506 mg of the polymer. $\overline{M}_n$ from conversion was 14 kDa. $\overline{M}_n$ from GPC-LS 19 kDa with a PDI of 1.09.

2.3. Release Studies

RBV release was quantified by chromatographing the samples by HPLC (Shimadzu LC-2010A HT). The column (Ascentis express C18, 15 cm × 3 mm) was equilibrated with the corresponding release buffer (pH = 7.4) or ultra pure water (pH = 1) as mobile phase at a flow rate of 0.4 mL min^{-1}. UV-Vis absorbance was monitored on a photo array detector (Shimadzu SPD-M20A). RBV was subsequently quantified at its absorption maximum (205 nm) against an external standard curve.

2.4. Cell Uptake

Hep G2 cells (50 000 cells per well, 100 μL media) and RAW264.7 macrophages (20 000 cells per well, 100 μL media) were seeded in 96-well plates for pre-incubation in 24 h. Then, media was changed (90 μL) and polymers (10 μL) were added in different concentrations and incubated (24 h). Then, the cells were trypsinized using Trypsin-EDTA 0.05% and analyzed by flow cytometry.

2.5. Cell Viability

Hep G2 cells (50 000 cells per well, for 24 h, 20 000 cells per well for 48 h and 10 000 cells per well for 72 h, 100 μL media) and RAW264.7 macrophages (20 000 cells per well for 24 h, 10 000 cells per well for 48 h and 5000 cells per well for 72 h, 100 μL media) were seeded in 96-well plates for pre-incubation (24 h). Then, media (90 μL) was changed and polymers (10 μL) were added in different concentrations and incubated (24, 48 and 72 h), followed by addition of CCK-8 (10 μL, 1 h) and absorbance was determined by EnSpire Multimode Plate Reader (450 nm). Negative control: 10 μL PBS. Positive control: 50% DMSO.

2.6. RBC Association and Hemolysis

Human RBCs obtained from Skejby Hospital blood bank were washed and mixed with cryopreservative (54.7 mM glycerol, 0.050 M $NaPO_3$, 0.37×10^{-3} M NaCl)[48] and stored at –80 °C.

RBC was thawed in a 37 °C water bath and subsequently washed with PBS (3× 10 mL, 5 min, 800 rpm). Then polymers (5 μL) were added to the RBC suspension (45 μL) in Eppendorf tubes and the samples were incubated overnight while shaken (37 °C, 300 rpm). Blank: untreated cells. Negative control: cells with PBS. Positive control: 50% Milli-Q water. After incubation, PBS was added without re-suspension of the samples, and following centrifugation (5 min, 800 rpm), 200 μL of the supernatant was transferred to a 96-well plate for UV-Vis absorbance measurements (541 nm). The remaining sample was washed with PBS (1× 1 000 μL, 5 min, 800 rpm), RBCs were suspended in PBS (1:2000 in PBS) and analyzed by flow cytometry.

2.7. RBC Aggregation

RBCs were thawed in a 37 °C water bath and subsequently washed with PBS (3× 10 mL, 5 min, 800 rpm). Then the RBCs were diluted in PBS (1:225), and polymers (10 μL) were added to the RBC suspension (90 μL) in Eppendorf tubes and the samples were incubated overnight while shaken (37 °C, 300 rpm). Blank: untreated cells. After incubation, the samples were washed with PBS (1× 1000 μL, 5 min, 800 rpm), supernatant was removed, and the remaining cells were suspended in PBS (200 μL) and analyzed by flow cytometry.

2.8. Inhibition of Nitric Oxide Synthesis

RAW264.7 macrophages (20 000 cells per well, 100 μL media) were seeded in 96-well plates. After 4 h, respective concentrations of polymers and L-N^G-nitroarginine methyl ester (L-NAME) were added. Following incubation (24 h), media was renewed and cells were stimulated through the addition of 1 μg mL^{-1} lipopolysaccharide (LPS, *Escherichia coli* 026:B6). After incubation (24 h), relative nitric oxide levels were determined by measuring nitrite levels through the Griess assay. In short, 50 μL media was transferred to a new 96-well plate and 50 μL sulphanilic acid (10 g L^{-1}, 5% phosphoric acid) were added. After incubation (5 min), 50 μL *N*-1-napthylethylenediamine dihydrochloride (1 g L^{-1}) was added and incubated (5 min), where after absorbance was measured using EnSpire Multimode Plate Reader (548 nm). The nitrite levels were quantified against a freshly prepared sodium nitrite standard curve and normalized within each experiment against the negative control consisting of LPS stimulated cells without the addition of any reagent/polymer. Viability of the cells was measured by quantifying metabolic activity through the

PrestoBlue assay according to the manufacturer's instructions. Each viability experiment was normalized against a negative control where no reagent/polymer/LPS had been added to the cells. Positive control: 20% DMSO.

2.9. Statistical Analysis

Student's *t*-test was applied to determine statistical significance using Excel software. One-tailed unpaired *t*-test with 95% confidence interval was considered statistical significant if $p < 0.05$ (*), $p < 0.01$ (**), and $p < 0.001$ (***).

3. Results and Discussion

3.1. Synthesis

Controlled radical polymerization is a powerful technique for the synthesis of MPs, in that it delivers a diversity of polymer properties achieved through the choice of constituting monomers, and it ensures close control over molecular weight and polydispersity of the formulations. These characteristics together define the pharmacokinetics of newly synthesized prodrugs. To be considered in the design of MPs, drug-derived monomers have to be amenable for controlled radical polymerization and allow hydrolytic, enzymatic or other mechanism of drug release. For nucleoside analogues and RBV in particular, synthetic opportunities in monomer design are rather limited. To our knowledge, the only previous example of RBV derived monomer was based on vinyl esters,[49] of which free radical polymerization afforded (co)polymers with polydispersity indexes of 2.26–2.50. Adipic vinyl ester of RBV has been used in a drug delivery scheme,[18] and shown to afford release of RBV via hydrolytic degradation. While successful, this synthetic scheme offers a poor control over macromolecular characteristics of the polymers. Further, it suffers from that only a limited number of monomers can be used for production of copolymers thus presenting only a narrow macromolecular space for structure-function analysis, optimization of drug carriers, etc. In contrast, synthesis of (meth)acrylate derivatives would greatly extend the applicability of RBV monomers with regard to potential co-monomers. In this work, synthesis of RBV acrylate was accomplished in a one-step enzymatic reaction using *Candida antarctica lipase* 435, in a procedure adapted from Moris and Gotor,[50] Scheme 1. This reaction proved selective for the 5'-hydroxyl, and offered a fast workup by filtration and precipitation, and in doing so facilitated gram-scale synthesis of RBV acrylate. Synthesis of RBV adipate was accomplished via an analogous protocol. We note that (enzymatic) synthesis of nucleoside based (meth)acrylates is now a well-established technique and examples of polymers derived thereof are many.[51,52] However, to the best of our knowledge, this strategy has not been previously adopted for the synthesis of MPs of nucleoside analogues, the latter being potent drugs in anticancer and antiviral therapies.

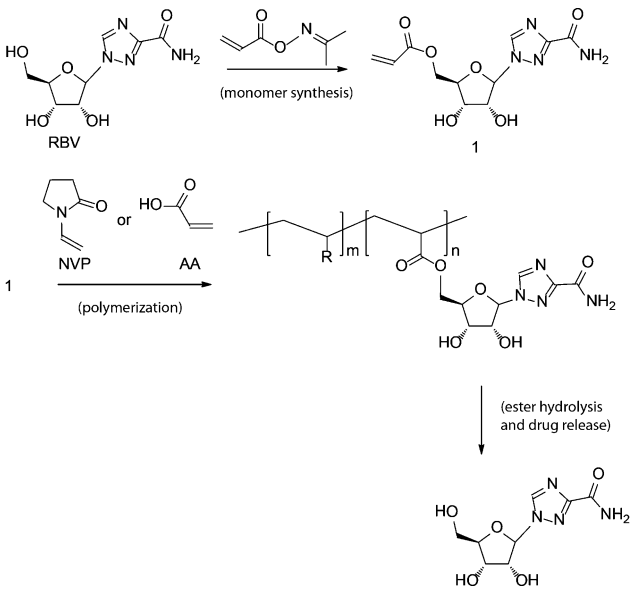

Scheme 1. Schematic illustration of the proposed synthesis of MPs of ribavirin (RBV). Polymerizable acrylate form of RBV was synthesized via a chemi-enzymatic approach using Nz435/CAL-B in dioxane, and used in RAFT polymerization with NVP and AA as comonomers to obtain MPs. R represents either NVP or AA as polymer backbone. Phthalimidomethyl-*O*-ethyl xanthate and cyanomethyldodecyl trithiocarbonate were employed as RAFT agent for PVP and PAA synthesis, respectively (see Supporting Information, Figure S1) Synthesized polymers released pristine RBV upon ester hydrolysis, both in test tubes at acidic conditions (as verified via HPCL/MS) and upon cellular internalization of the prodrugs, in the latter case resulting in a pronounced therapeutic response.

Polymerization of NVP and RBV acrylate was performed in DMSO, a solvent suitable from the standpoint of solubility of the nucleoside containing monomer and also compatibility with RAFT. While optimizing reaction conditions, it was observed that regardless of feed ratios, conversion of RBV acrylate was near complete regardless of conversion of NVP. In contrast, NVP conversion remained low and decreased with increasing RBV feed. Increased content of RBV acrylate in the monomer mixture was also detrimental as to the quality of the resulting polymers, that is, polydispersity indexes. These data are rather expected and reflect the notion that these two monomers require dissimilar RAFT agents for controlled (co)polymerizations. In this work, we used a xanthate RAFT agent suitable for NVP, and allowed near un-controlled polymerization of the acrylate. With low feed of RBV acrylate, however, the polymers obtained revealed acceptable polydispersity and molecular weight. The rapid conversion of RBV acrylate as compared to NVP suggests that the resulting copolymer

may have a higher content of RBV in the proximity of the R terminus.

For acrylic acid, co-polymerization with RBV acrylate was conducted in DMF following procedures reported elsewhere.[53] In contrast to above discussed copolymerizations with NVP, increased feed of RBV acrylate did not inhibit polymerization of AA, as would be expected with the overall compatibility of the co-monomers and the RAFT agent. This afforded predictable results and incorporation of RBV in the polymer similar to the feed ratio of monomers in the polymerization. Macromolecular characteristics of RBV based PVP and PAA co-polymers are listed in Table 1. Both PVP and PAA based copolymers contained a fraction of fluorescein acrylate to accommodate subsequent analyses of cellular association and internalization via fluorescence based techniques, namely flow cytometry. We note that details of optimization of polymerization reactions as well as structure-function relationship with regard to macromolecular characteristics of these prodrugs will be reported in a separate publication. In this work, we report proof-of-concept MPs of RBV and gain the first insight into their utility in delivery of this broad-spectrum antiviral agent.

3.2. Hemocompatibility of Macromolecular Prodrugs

Ribavirin is known to result in hemolytic anaemia, which is a result of unspecific accumulation of the agent in RBCs.[54] The concentration of RBV within the erythrocytes may exceed that in the blood stream by as much as 100-fold.[55] The latter phenomenon is responsible for an astounding value of volume of distribution for RBV, of 2000 L.[12] This notion implies that only a minor fraction of administered drug is responsible for the therapeutic benefit. It is well documented in the state of art, that cationic polymers exhibit association with RBCs; in contrast, non-ionic and negatively charged polymers exhibit a low level of association with erythrocytes. This led us to hypothesize that conjugation of RBV with an appropriate carrier polymer would prevent the drug from entering RBCs. In doing so, we aimed to address the major side effect of this broad spectrum antiviral and facilitate distribution of the drug towards the target tissue, namely the liver.

Polymer association with erythrocytes was monitored using isolated RBCs and flow cytometry as a method of analysis, Figure 1. Polymer samples were synthesized with a fraction of fluorescein acrylate in the monomer feed thus affording fluorescently labeled polymers. Upon incubation with RBCs, increase in the cell fluorescence as registered through flow cytometry indicates association of the polymer chains with erythrocytes (Figure 1i). We note that while flow cytometry does not distinguish between association and internalization of cargo by cells, erythrocytes do not exhibit endocytotic uptake typical of mammalian cells,[56] and are thought not to internalize administered polymers. It is therefore most likely that revealed increase in cell fluorescence is due to polymer association with the cell membrane without cell entry. Raw experimental data on fluorescence of individual cells as attained depending on the concentration of the polymer in the incubation media, Figure 1i, were used to estimate the fraction of cells with associated polymer chains, Figure 1ii. To achieve this, un-treated cells were used to set the gating so that ≈5% of cells exhibit fluorescence above a threshold level of fluorescence. Upon polymer binding, cells exhibit increased fluorescence and are counted as positive for associated polymer if the attained level of fluorescence exceeded the nominated threshold. This arbitrary method is standard in flow cytometry and is highly sensitive to variation in fluorescence of polymer chains. To facilitate analysis and avoid erroneous conclusions, here and throughout the paper flow cytometry mean fluorescence data were analyzed with due normalization using relative fluorescence of the synthesized polymers (Table 1).

At polymer concentrations 1–10 $\mu g\,mL^{-1}$ and a 24 h incubation time, polymers exhibited a non-detectable degree of association with erythrocytes, as evidenced by a minimal level of fluorescence of individual cells, Figure 1ii. At increased polymer concentration (100 $\mu g\,mL^{-1}$), cells

Table 1. Macromolecular characteristics of the synthesized macromolecular prodrugs.

	PVP		PAA	
RBV feed [%]	0.7	0	5	0
Conversion [% RBV]	100	–	70	–
Conversion [% NVP or AA]	35	43	68	63
RBV [mol%]	3	–	4.5	–
Mn [kDa]	17	15	27	19
PDI	1.13	1.7	1.16	1.09
Fluorescence [a.u.]	1.5	1	2.3	2

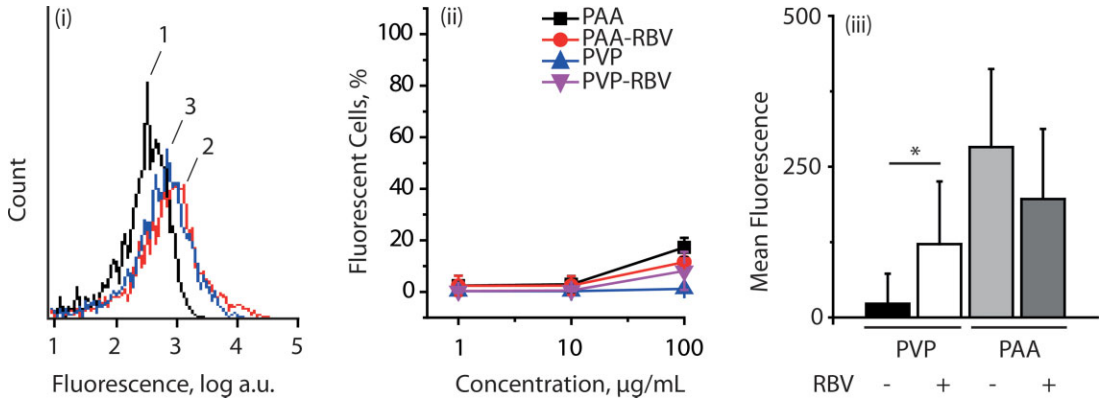

Figure 1. i) Histogram showing fluorescent intensity of untreated erythrocytes (1) and erythrocytes upon their incubation with PAA (2) and PAA-RBV (3); ii) association of PAA, PAA-RBV, PVP and PVP-RBV with erythrocytes after 24 h incubation as studied by flow cytometry; iii) mean fluorescence of erythrocytes upon their incubation with MPs at 100 μg mL^{-1} concentration of the polymers over 24 h at 37 °C. For experimental details, see main text and experimental section. Results shown are average of triplicate experiments, reported as mean ± SD ($n = 3$). * $p < 0.05$.

exhibited a certain increase in fluorescence (Figure 1iii), indicating possible association of polymers with the erythrocytes, however, average cell fluorescence only increased by 200–300 arbitrary units. Compared to registered increase in fluorescence upon association and/or internalization of these polymers by mammalian cells with hepatic relevance (see below), increase in fluorescence for RBCs was well below 1%. This notion illustrated the success of the chosen approach to overcome the origin of the main side effect of RBV, namely accumulation in erythrocytes.

For a broader analysis of the synthesized MPs, polymer-induced aggregation of erythrocytes, that is, hemagglutination, a phenomenon highly un-desirable for implementation of RBV containing MP as polymer therapeutics, was monitored. This effect is known to be brought about by polycations whereas neutral polymers, for example, PEG, are commonly used to prevent aggregation of erythrocytes induced by positively charged (co)polymers.[57] Learning from our prior work on polymer-induced aggregation of microparticles,[58] quantification of RBC agglutination was performed using flow cytometry, specifically light scattering parameters. For pristine erythrocytes (Figure 2i), and erythrocytes in the presence of polymers taken at the highest concentration studied (100 μg mL^{-1}, Figure 2ii), flow cytometry light scattering plots were similar and therefore reveal a minimal if any tendency of the cells to aggregate. This observation is highly important and reveals that polymer association with the RBCs does not lead to a loss of colloidal stability of the latter.

Another plausible effect of polymer interaction with RBCs is that of hemolysis, that is, degradation of erythrocytes by the interacting polymer chains. Hemocompatibility is a highly important aspect of polymers for biomedical applications, and has typically been assessed in the context of, for example, gene delivery to ascertain side effects due to the membrane associative properties of polycations. From a different perspective, it has also been shown that hydrophobic analogues of PAA, namely poly

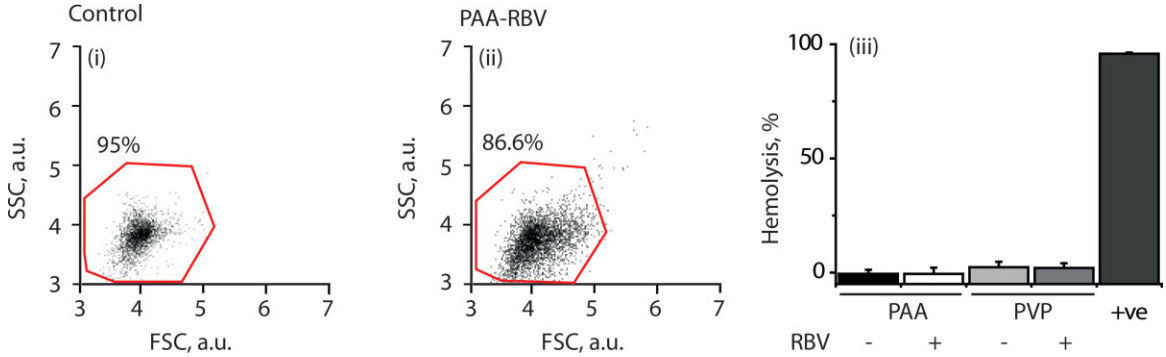

Figure 2. i,ii) Flow cytometry FSC/SSC dot plots for i) pristine erythrocytes and ii) erythrocytes upon incubation with PAA-RBV at 100 μg mL^{-1} over 24 h at 37 °C; iii) hemolysis of erythrocytes upon incubation with PAA, PAA-RBV, PVP, and PVP-RBV at 100 μg mL^{-1} over 24 h at 37 °C, positive control (+ve) in 50% Milli-Q water. Results shown are average of triplicate experiments, reported as mean ± SD ($n = 3$).

ethyl- and propylacrylic acids, have membranolytic properties and can cause lysis of erythrocytes.[59] To ascertain hemocompatibility for RBV containing PVP and PAA, stability of erythrocytes in the presence of administered polymers was analyzed using UV-Vis based analysis, in which release of hemoglobin was used as an indicator of compromised integrity of erythrocytes.[59,60] Hemolysis was assessed following a 24 h incubation of RBCs with 100 μg mL^{-1} polymer under constant shaking at 37 °C. None of the formulations resulted in measurable release of hemoglobin, thus indicating minimal hemolysis, Figure 2 (iii). Taken together, the data in Figure 1 and 2 provide multi-angle ex vivo validation of hemocompatibility of the synthesized MPs of RBV. Our data demonstrate that RBV-functionalized polymers have a minimal tendency to associate with RBCs, a phenomenon which is poised to alleviate the most well documented side effect of ribavirin, namely accumulation in RBCs. To our knowledge, this study is the first of its kind and presents a novel tool to overcome the dose-limiting side effect of RBV.

3.3. Polymer Interaction with Hepatic Cells

As an initial test for utility of the synthesized co-polymers in delivery of RBV, we investigated interaction of the synthesized MPs with mammalian cells with hepatic relevance, namely hepatocytes, Hep G2 and macrophages, RAW264.7. The latter are used herein as model cell line for Kupffer cells,[61] liver resident macrophages. In all experiments, cells were allowed 24 h for initial adhesion, after which media was exchanged, and solutions of polymers were administered to cultured cells to a final concentration of 100 μg mL^{-1}. Following further incubation (1 or 24 h), cells were harvested via trypsinization, washed with PBS, and analyzed using flow cytometry. Figure 3 shows representative experimental data obtained for PAA-based polymer therapeutics as histograms of fluorescence of individual cells. For hepatocytes, association and/or internalization of the polymers was well-pronounced and rather fast, as evident from a significant increase in the levels of cells fluorescence (≈100-fold) achieved within 1 h of incubation, as well as similarity of the histograms obtained after 1 and 24 h incubation of cells with the polymers. It can also be noted, qualitatively, that polymers with and without RBV exhibit a similar level of cellular internalization. For macrophages (Figure 3iii,iv), the data were similar in that levels of fluorescence acquired by cells upon incubation with PAA and PAA-RBV were near identical, that is, RBV-containing PAA was internalized to a similar extent as a pristine PAA polymer. However, significant difference between macrophages and hepatocytes was evident in that polymer association and/or internalization in macrophages was markedly slower. After 1 h of incubation with polymers (Figure 3iii), macrophages

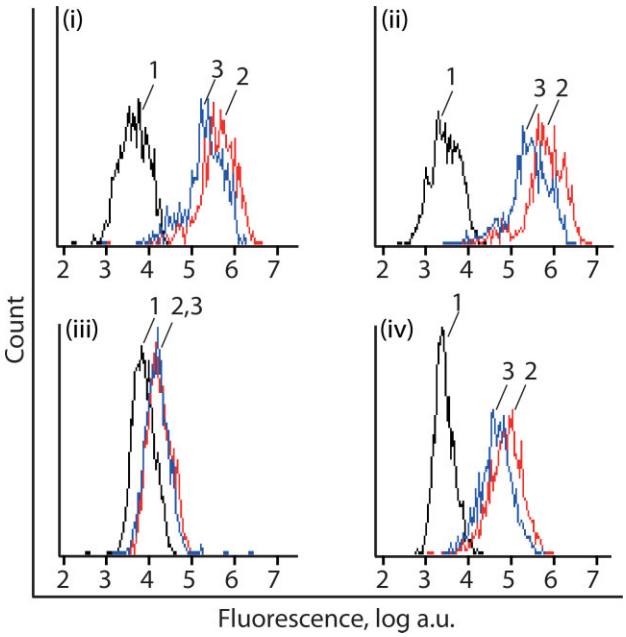

Figure 3. Experimental data on fluorescence of the cells (i, ii: hepatocytes; iii, iv: macrophages) upon their incubation with PAA and PAA-RBV at polymer concentrations 100 μg mL^{-1} over 1 h (i, iii) or 24 h (ii, iv). Each graph shows data for untreated cells (1) and cells upon their incubation with PAA (2) and PAA-RBV (3).

revealed a minor shift in the fluorescence intensity, yet upon 24 h incubation, fluorescence intensity of these cells was significantly higher than that of untreated cells (Figure 3iv). We acknowledge that flow cytometry does not distinguish between cell surface association and internalization of cargo, and this notion complicates analyses of drug delivery using, for example, microcapsules and microparticles. For brevity, here and below we attribute increase in hepatocytes and macrophages fluorescence to polymer internalization and admit that surface association of co-polymers cannot be ruled out. Detailed investigation of surface binding versus internalization of co-polymers exceeds the scope of this initial investigation. However, intracellular mode of action of RBV, as well as a revealed therapeutic response (see below), strongly suggests a pronounced level of polymer internalization.

Fluorescence of harvested cells was quantified upon incubation with polymers at different concentrations ranging from 0.1 to 100 μg mL^{-1}, Figure 4. Both hepatocytes and macrophages exhibited a dose-dependent internalization of PAA and its RBV functionalized counterpart. Polymer uptake was noticeable at administered concentration as low as 1 μg mL^{-1}, as shown by an increase in the cells fluorescence. Uptake was significantly more pronounced at 10 μg mL^{-1} polymer concentration, with the exception of polymer uptake by macrophages during 1 h incubation. At a concentration of 100 μg mL^{-1} and 24 h

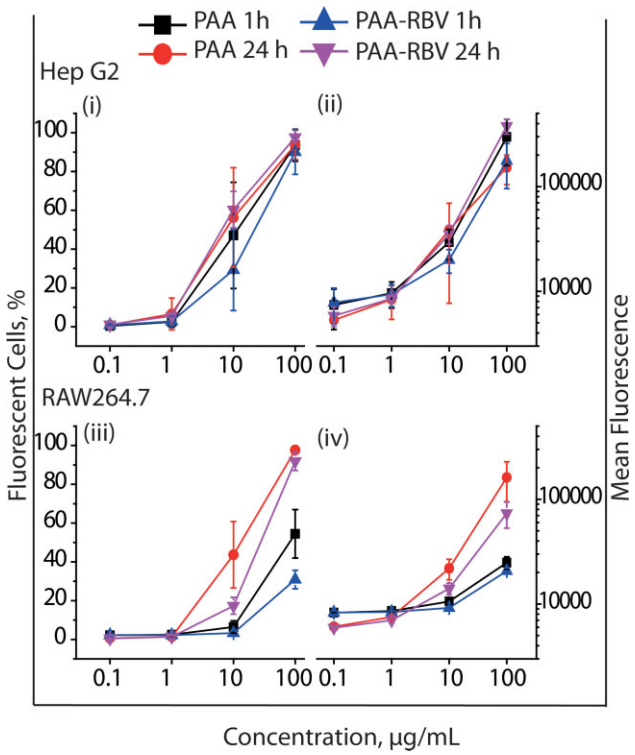

Figure 4. i,iii) Percent fluorescent cells and ii,iv) mean population fluorescence for hepatocytes (top) and macrophages (bottom) upon their incubation with PAA and PAA-RBV over 1 or 24 h at polymer concentrations from 0.1 to 100 $\mu g \cdot mL^{-1}$. Results shown are the average of triplicate experiments, reported as mean ± SD ($n = 3$).

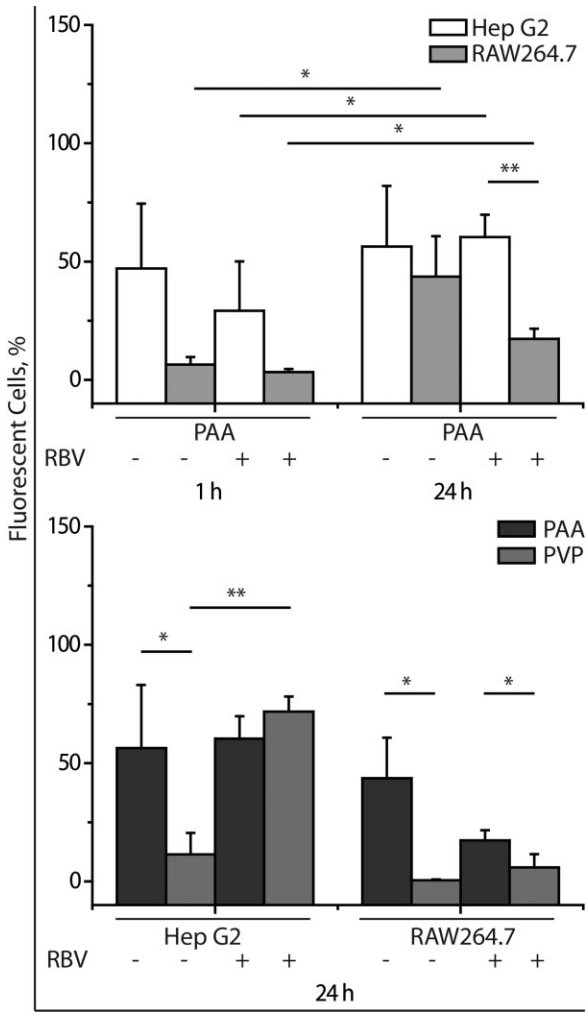

Figure 5. Statistical evaluation of experimental data on the interaction of the synthesized polymers with hepatocytes and macrophages at polymer concentration 10 $\mu g\,mL^{-1}$ over 1 or 24 h of incubation. Results shown are the average of triplicate experiments, reported as mean ± SD ($n = 3$). $^{*}\ p < 0.05$ $^{**}\ p < 0.01$ $^{***}\ p < 0.001$.

incubation, both hepatocytes and macrophages revealed a near quantitative population shift, i.e., most cells tested positive for polymer fluorescence. At each polymer concentration, interaction of macrophages with the polymers was time delayed, a trend which was not observed for hepatocytes. It should be noted that for brevity, only data for PAA and RBV-containing PAA are shown in Figure 4. Monitoring cell uptake for PVP and PVP-RBV yielded qualitatively similar observations (data not shown).

We next performed a multi-angle statistical evaluation of the data. Conclusions drawn were typically consistent for analyses using per cent fluorescent cells and mean fluorescence as parameters of comparison. For brevity, only the main points are discussed below with an overall graphical representation of sample-to-sample evaluations presented in Figure 5 and in Supporting Information. For PVP, the presence of RBV compromised the low fouling properties of the polymer. This phenomenon manifests itself through drastically increased polymer internalization by hepatocytes and macrophages which was evident by increased fraction of cells with acquired fluorescence, as well as an overall average level of fluorescence for the cells population. In contrast, no such trend was observed for PAA polymers, and in most cases uptake of PAA-RBV was comparable to that of pristine PAA. This notion was further reflected by the analysis of polymer-to-polymer variation in cellular internalization (e.g., 24 h incubation time, 10 $\mu g\,mL^{-1}$ polymer concentration). For hepatocytes, pristine PAA exhibited an increased uptake compared to pristine PVP to a level which cannot be explained by differences in fluorescent labeling of the two polymers (Table 1). In other words, PVP exhibited an expected low fouling behavior. In contrast, for RBV containing prodrugs, the trend was reverse and PAA-RBV revealed internalization to a lower extent that PVP-RBV. Interestingly, with macrophages the above observation was far less pronounced and a difference in

cellular internalization of PVP-RBV and PAA-RBV was relatively minor. Time of incubation as a tool of control of polymer internalization had a rather expected result, and for both cell lines extended incubation time resulted in an increased level of cells fluorescence. However, for macrophages this effect was well pronounced, and percent fluorescent cells registered upon incubation with 100 $\mu g\,mL^{-1}$ of PAA-RBV increased from ≈30 to over 90% from 1 to 24 h incubation. With the same conditions, percent of Hep G2 cells increased only marginally, from 90 to ≈100%. Finally, cell-to-cell comparison revealed that for both PAA- and PVP-based MPs (1 or 24 h incubation time, 10 $\mu g\,mL^{-1}$ polymer concentration) uptake in hepatocytes was considerably increased as compared to macrophages.

Taken together, the above data present PVP and PAA as polymer carriers for hepatic delivery of RBV. The most important observation from Figure 1–5 was that there existed a wide window of polymer concentrations at which hepatic cells lines exhibited a pronounced uptake of polymer therapeutics whereas RBCs revealed no association with the administered polymers. In other words, our data provide an ex vivo validation to the proposed concept whereby conjugating RBV to polymer chains alleviates the most significant side effect of RBV, namely accumulation in the RBCs. We strongly believe that this is the first example of tools of polymer therapeutics applied to optimize pharmacokinetics of RBV, a broad spectrum antiviral drug.

3.4. Cytotoxic and Therapeutic Effects

Aiming to use the synthesized prodrugs in intracellular drug delivery, we next evaluated cytotoxicity of the RBV-containing copolymers. In preliminary experiments we verified that the synthesized prodrugs release pristine RBV upon hydrolysis of the ester functionality. This was accomplished via incubation of the polymers in acidified aqueous environment to promote ester hydrolysis, and degradation products were analyzed using HPLC and mass spectrometry. These tests confirmed that the polymers release RBV (m/z $[M+H^+]$ calculated for RBV, $C_8H_{13}N_4O_5$: 245.0880; found: 245.0878) thus, verifying the concept of MPs of this broad spectrum antiviral agent as put forward in this work.

Previous studies have shown that to manifest toxicity, RBV and RBV-containing polymers may require up to 72 h incubation time with mammalian cells.[18,62] In this work, potential polymer toxicity was evaluated for an entire range of polymer concentrations and analysis was conducted in 24–72 h. Representative results are shown in Figure 6. Metabolic activity of hepatocytes and macrophages showed minimal decrease in the presence of PAA and PVP based copolymers, as verified using CCK-8 viability

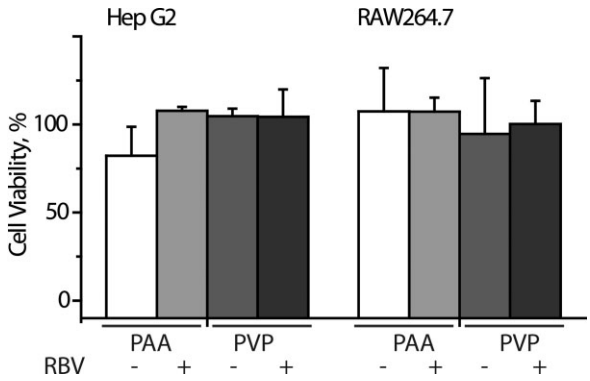

Figure 6. Cell viability of hepatocytes and macrophages incubated with the synthesized polymers at concentration 10 $\mu g\,mL^{-1}$ over 72 h. Results shown are the average of triplicate experiments, reported as mean ± SD ($n = 2$). Positive control: 50% DMSO.

assay. This observation strongly suggested that MPs as synthesized in this work and administered using indicated concentrations and incubation times do not afford a build-up of intracellular concentration of RBV to a toxic level. We note that past studies have used cytotoxicity as a read out to substantiate intracellular drug release.[18] However, cytotoxicity of antiviral drugs, as well as their MPs, is an un-desired effect and as such should be avoided. This notion highlights attractiveness of the synthesized prodrugs for delivery of ribavirin.

An added challenge to the development of prodrugs of RBV is that despite 40 years of successful history in medicinal uses, biochemical mechanism of action of this drug against HCV is still a subject of debate.[6] In contrast to typical nucleoside analogues, RBV has been hypothesized to exert an immuno-modulating effect rather than a direct antiviral action.[6] This notion led us to investigate intracellular processes and metabolic pathways which may be affected by RBV. Literature survey revealed a hypothesis that RBV exerts a therapeutic effect via an indirect inhibition of activity of inducible nitric oxide synthase (iNOS),[63] that is, has an anti-inflammatory action in liver resident macrophages, Kupffer cells. Surprisingly, to the best of our knowledge, the effect of RBV on NOS has only been quantified in a single report, in human umbilical vein endothelial cells with relevance to angiogenesis,[64] and, with exception of our recent communication on the subject,[46] remains un-explored in macrophages. In this work, macrophages were exposed to bacterial LPS to induce intracellular production of iNOS and release of nitric oxide. The cells were than used to quantify the effect elicited by RBV, for which purpose relative concentrations of NO in the supernatants above cultured cells were quantified via the Griess assay.[65] We used a concentration of RBV closely matching therapeutic concentrations of this antiviral drug, 10 μM

RBV.[66] Remarkably, supporting the hypothesis put forward, this treatment afforded a ≈50% inhibition of nitric oxide release, indicating a pronounced anti-inflammatory activity of this nucleoside analogue, Figure 7. However, drug exposure also resulted in a statistically significant decrease in cell viability (≈20%) reflecting a narrow therapeutic window of RBV in this treatment. We strongly emphasize that this result appears to be the first experimental proof of iNOS inhibition by RBV in macrophages. Furthermore, revealed effect is well-pronounced at a concentration of RBV typically used in anti-HCV treatment and this strongly suggests that anti-iNOS activity manifests itself in clinical applications of ribavirin. A detailed investigation of the anti-inflammatory activity of RBV will be subject of our upcoming publications.

In the absence of conjugated drug, PVP and PAA elicited minor if any effect on the production of NO by stimulated macrophages. In contrast, RBV-containing counterparts proved to be highly effective and at the highest concentration tested, both PVP-RBV and PAA-RBV exhibited a pronounced, statistically significant ability to suppress production of NO. Furthermore, for PAA-RBV, efficacy of treatment was comparable to that of non-conjugated RBV. While it is highly unlikely that both, an entire administered dose is internalized by cells and an entire payload of RBV is released from a polymer chain, our data strongly suggest a successful intracellular release of a fraction of RBV from the MPs. Indeed, intracellular activity of RBV is dependent on phosphorylation on the 5′ hydroxyl,[67] that is, the same hydroxyl used for the synthesis of RBV monomer and the MP, which implies separation of the drug from its polymer carrier. What appears to be the most significant observation is that when in the form of polymer conjugate, delivery of RBV to the stimulated macrophages and intracellular anti-inflammatory activity was associated with a negligible cytotoxic effect, in stark contrast to pristine RBV. The data in Figure 7 therefore verify a novel intracellular target for activity of RBV, and present MPs of RBV as fine tools for controlled drug delivery. We believe that these data are the first examples of RBV-containing synthetic MPs with documented therapeutic benefit.

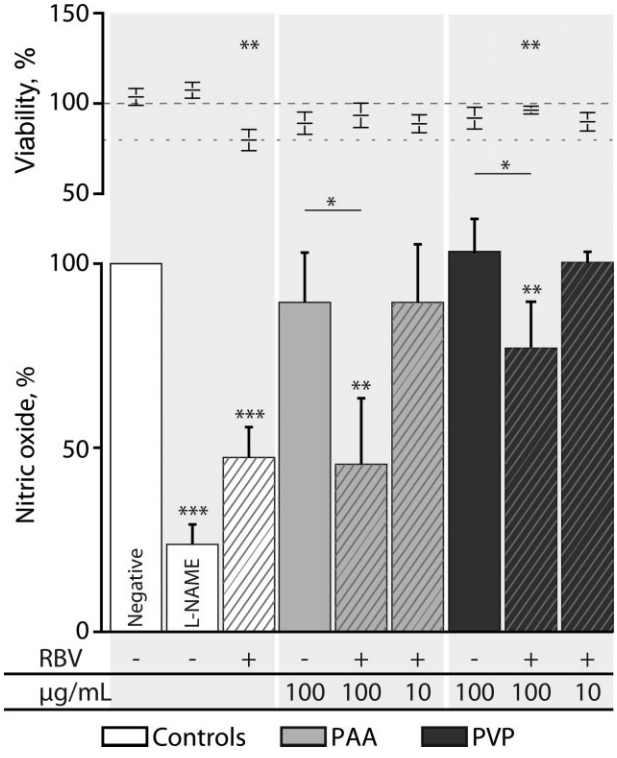

Figure 7. Ribavirin (10 μM), L-NAME (1 mM, iNOS inhibitor), and the synthesized polymeric prodrugs at concentration 10 and 100 μg mL^{-1} were pre-incubated (24 h) with macrophages, followed by LPS stimulation. After 24 h relative NO levels and cellular viability were quantified. Results shown are average of three independent experiments, reported as mean ± SD ($n = 3$). Statistical significance is given in relation to the negative control, if not indicated otherwise. * $p < 0.05$, ** $p < 0.01$, *** $p < 0.001$.

4. Conclusion

Data presented in this work demonstrate that MPs of ribavirin constitute a powerful tool to achieve a safer delivery of this broad spectrum antiviral agent. Conjugation to a carrier polymer prevents association of the drug with the RBCs and in doing so overcomes the origin of the main side effect of RBV. Polymer therapeutics based on PVP and PAA exhibited no hemolysis or erythrocyte aggregation behavior in vitro thus, further validating hemocompatibility of the newly synthesized MPs. While association with erythrocytes was suppressed, interaction

of MPs with mammalian cells with hepatic relevance was pronounced. In hepatocytes and macrophages, MPs revealed negligible cytotoxicity speaking towards biocompatibility of these formulations. A significant finding of this work for broader biomedical sciences is that RBV exerts a pronounced anti-inflammatory effect, specifically through inhibition of synthesis of NO in macrophages. At concentrations closely matching therapeutically relevant, treatment with RBV resulted in a 50% reduction in the levels of NO, but also exhibited a statistically significant cytotoxic effect. MPs revealed a matching efficacy of treatment and this effect, remarkably, was not associated with cytotoxicity. We strongly believe that presented data contribute significantly to the development of polymer therapeutics for delivery of antiviral drugs.

Acknowledgements: RAW264.7 cells were a generous of gift from Søren Kragh Moestrup laboratory, Aarhus University. Erythrocytes were supplied generously by the Skejby Hospital blood bank. Thomas Hussmann (Aarhus University) is acknowledged for laboratory assistance. This work is supported by a grant from the Lundbeck Foundation and Sapere Aude Starting Grant from the Danish Council for Independent Research, Technology and Production Sciences, Denmark.

Received: May 19, 2013; Revised: August 5, 2013; Published online: September 17, 2013; DOI: 10.1002/mabi.201300244

Keywords: antiviral therapy; hepatitis; inflammation; polymer therapeutics; ribavirin

[1] WHO, http://www.who.int/mediacentre/factsheets/fs164/en/index.html **2012**.
[2] M. K. Jain, C. Zoellner, *Expert Opin. Pharmacother.* **2010**, *11*, 673.
[3] J. Y. N. Lau, R. C. Tam, T. J. Liang, Z. Hong, *Hepatology* **2002**, *35*, 1002.
[4] R. W. Sidwell, J. H. Huffman, G. P. Khare, L. B. Allen, J. T. Witkowski, R. K. Robins, *Science* **1972**, *177*, 705.
[5] J. L. Patterson, R. Fernandez-Larsson, *Rev. Infect. Dis.* **1990**, *12*, 1139.
[6] E. De Clercq, *Nat. Rev. Drug Discovery* **2007**, *6*, 1001.
[7] M. W. Fried, *Hepatology* **2002**, *36*, s237.
[8] W. B. Parker, *Virus Res.* **2005**, *107*, 165.
[9] L. De Franceschi, G. Fattovich, F. Turrini, K. Ayi, C. Brugnara, F. Manzato, F. Noventa, A. M. Stanzial, P. Solero, R. Corrocher, *Hepatology* **2000**, *31*, 997.
[10] P. G. Canonico, M. D. Kastello, C. T. Spears, J. R. Brown, E. A. Jackson, D. E. Jenkins, *Toxicol. Appl. Pharmacol.* **1984**, *74*, 155.
[11] B. E. Gilbert, V. Knight, *Antimicrob. Agents Chemother.* **1986**, *30*, 201.
[12] P. Glue, *Semin. Liver Dis.* **1999**, *19*, 17.
[13] R. Duncan, *Nat. Rev. Drug Discovery* **2003**, *2*, 347.
[14] J. Sanchis, F. Canal, R. Lucas, M. J. Vicent, *Nanomedicine* **2010**, *5*, 915.
[15] W. Li, Y. Chang, P. Zhan, N. Zhang, X. Liu, C. Pannecouque, E. De Clercq, *ChemMedChem* **2010**, *5*, 1893.
[16] W. J. Li, J. D. Wu, P. Zhan, Y. Chang, C. Pannecouque, E. De Clercq, X. Y. Liu, *Int. J. Biol. Macromol.* **2012**, *50*, 974.
[17] S. Brookes, P. Biessels, N. F. L. Ng, C. Woods, D. N. Bell, G. Adamson, *Bioconjugate Chem.* **2006**, *17*, 530.
[18] X. Li, Q. Wu, M. Lu, F. Zhang, X. F. Lin, *J. Polym. Sci. Part A: Polym. Chem.* **2008**, *46*, 2734.
[19] X. Li, Q. Wu, Z. Chen, X. Gong, X. Lin, *Polymer* **2008**, *49*, 4769.
[20] G. A. Levy, G. Adamson, M. J. Phillips, L. A. Scrocchi, L. Fung, P. Biessels, N. F. Ng, A. Ghanekar, A. Rowe, M. X. Z. Ma, A. Levy, C. Koscik, W. He, R. Gorczynski, S. Brookes, C. Woods, I. D. McGilvray, D. Bell, *Hepatology* **2006**, *43*, 581.
[21] R. Duncan, M. J. Vicent, *Adv. Drug Delivery Rev.* **2010**, *62*, 272.
[22] M. Barz, R. Luxenhofer, R. Zentel, M. J. Vicent, *Polym. Chem.* **2011**, *2*, 1900.
[23] W. H. Amspacher, I. Gray, *Ann. N. Y. Acad. Sci.* **1952**, *55*, 526.
[24] A. L. Nielsen, K. Steffensen, K. L. Larsen, *Colloid Surf., B* **2009**, *73*, 267.
[25] S. D. Ren, D. Y. Chen, M. Jiang, *J. Polym. Sci., Part A: Polym. Chem.* **2009**, *47*, 4267.
[26] M. A. Gauthier, M. I. Gibson, H. A. Klok, *Angew. Chem., Int. Ed.* **2009**, *48*, 48.
[27] M. G. Tardajos, M. Nash, Y. Rochev, H. Reinecke, C. Elvira, A. Gallardo, *Macromol. Chem. Phys.* **2012**, *213*, 529.
[28] J. U. A. Engström, L. J. Lindgren, B. Helgee, *Macromol. Chem. Phys.* **2006**, *207*, 536.
[29] T. Trellenkamp, H. Ritter, *Macromolecules* **2010**, *43*, 5538.
[30] Y. Kaneda, Y. Tsutsumi, Y. Yoshioka, H. Kamada, Y. Yamamoto, H. Kodaira, S. Tsunoda, T. Okamoto, Y. Mukai, H. Shibata, S. Nakagawa, T. Mayumi, *Biomaterials* **2004**, *25*, 3259.
[31] S. Tsunoda, H. Kamada, Y. Yamamoto, T. Ishikawa, J. Matsui, K. Koizumi, Y. Kaneda, Y. Tsutsumi, Y. Ohsugi, T. Hirano, T. Mayumi, *J. Controlled Release* **2000**, *68*, 335.
[32] G. Pound, J. M. McKenzie, R. F. M. Lange, B. Klumperman, *Chem. Commun.* **2008**, 3193.
[33] M. Baba, D. Schols, E. De Clercq, R. Pauwels, M. Nagy, J. Györgyi-Edelényi, M. Löw, S. Görög, *Antimicrob. Agents Chemother.* **1990**, *34*, 134.
[34] A. Basu, T. Kanda, A. Beyene, K. Saito, K. Meyer, R. Ray, *J. Virol.* **2007**, *81*, 3933.
[35] J. Rojo, R. Delgado, *J. Antimicrob. Chemother.* **2004**, *54*, 579.
[36] M. Baba, R. Pauwels, J. Balzarini, J. Arnout, J. Desmyter, E. De Clercq, *Proc. Nat. Acad. Sci.* **1988**, *85*, 6132.
[37] A. Bernkop-Schnurch, *Adv. Drug Delivery Rev.* **2005**, *57*, 1569.
[38] M. Rutnakornpituk, N. Puangsin, P. Theamdee, B. Rutnakornpituk, U. Wichai, *Polymer* **2011**, *52*, 987.
[39] V. Thilakarathne, V. A. Briand, Y. X. Zhou, R. M. Kasi, C. V. Kumar, *Langmuir* **2011**, *27*, 7663.
[40] S. V. Kazakov, V. I. Muronetz, M. B. Dainiak, V. A. Izumrudov, I. Y. Galaev, B. Mattiasson, *Macromol. Biosci.* **2001**, *1*, 157.
[41] J. M. Pelet, D. Putnam, *Bioconjugate Chem.* **2011**, *22*, 329.
[42] V. A. Kabanov, *Pure Appl. Chem.* **2004**, *76*, 1659.
[43] A. V. Kabanov, *Adv. Drug Delivery Rev.* **2006**, *58*, 1597.
[44] M. A. C. Stuart, W. T. S. Huck, J. Genzer, M. Muller, C. Ober, M. Stamm, G. B. Sukhorukov, I. Szleifer, V. V. Tsukruk, M. Urban, F. Winnik, S. Zauscher, I. Luzinov, S. Minko, *Nat. Mater.* **2010**, *9*, 101.
[45] D. Roy, J. N. Cambre, B. S. Sumerlin, *Prog. Polym. Sci.* **2010**, *35*, 278.

[46] M. B. L. Kryger, B. M. Wohl, A. A. A. Smith, A. N. Zelikin, *Chem. Commun.* **2013**, *49*, 2643.
[47] J. Chiefari, Y. K. Chong, F. Ercole, J. Krstina, J. Jeffery, T. P. T. Le, R. T. A. Mayadunne, G. F. Meijs, C. L. Moad, G. Moad, E. Rizzardo, S. H. Thang, *Macromolecules* **1998**, *31*, 5559.
[48] S. Henkelman, G. Rakhorst, J. Blanton, W. van Oeveren, *Mater. Sci. Eng. C-Biomimet. Supramol. Syst.* **2009**, *29*, 1650.
[49] B. K. Liu, N. Wang, Q. Wu, C. Y. Xie, X. F. Lin, *Biotechnol. Lett.* **2005**, *27*, 717.
[50] F. Moris, V. Gotor, *J. Org. Chem.* **1993**, *58*, 653.
[51] A. Marsh, A. Khan, D. M. Haddleton, M. J. Hannon, *Macromolecules* **1999**, *32*, 8725.
[52] L. Zhang, W. G. Liu, L. Lin, D. Y. Chen, M. H. Stenzel, *Biomacromolecules* **2008**, *9*, 3321.
[53] A. Aqil, C. Detrembleur, B. Gilbert, R. Jérôme, C. Jérôme, *Chem. Mater.* **2007**, *19*, 2150.
[54] H. C. Bodenheimer, K. L. Lindsay, G. L. Davis, J. H. Lewis, S. N. Thung, L. B. Seeff, *Hepatology* **1997**, *26*, 473.
[55] Y. Inoue, M. Homma, Y. Matsuzaki, M. Shibata, T. Matsumura, T. Ito, Y. Kohda, *Hepatol. Res.* **2006**, *34*, 23.
[56] G. E. Palade, *J. Biophys. Biochem. Cytol.* **1955**, *1*, 567.
[57] B. I. Cerda-Cristerna, H. Flores, A. Pozos-Guillen, E. Perez, C. Sevrin, C. Grandfils, *J. Controlled Release* **2011**, *153*, 269.
[58] A. N. Zelikin, A. L. Becker, A. P. R. Johnston, K. L. Wark, F. Turatti, F. Caruso, *ACS Nano* **2007**, *1*, 63.
[59] E. F. Crownover, A. J. Convertine, P. S. Stayton, *Polym. Chem.* **2011**, *2*, 1499.
[60] N. Murthy, J. R. Robichaud, D. A. Tirrell, P. S. Stayton, A. S. Hoffman, *J. Controlled Release* **1999**, *61*, 137.
[61] E. Wisse, *J. Ultrastruct. Res.* **1974**, *46*, 393.
[62] S. Shigeta, S. Mori, M. Baba, M. Ito, K. Honzumi, K. Nakamura, H. Oshitani, Y. Numazaki, A. Matsuda, T. Obara, *Antimicrob. Agents Chemother.* **1992**, *36*, 435.
[63] R. E. Kast, *Neoplasia* **2003**, *5*, 3.
[64] M. Michaelis, R. Michaelis, T. Suhan, H. Schmidt, A. Mohamed, H. W. Doerr, J. Cinatl, Jr., *FASEB J.* **2007**, *21*, 81.
[65] M. J. Moorcroft, J. Davis, R. G. Compton, *Talanta* **2001**, *54*, 785.
[66] A. Tsubota, N. Akuta, F. Suzuki, Y. Suzuki, T. Someya, M. Kobayashi, Y. Arase, S. Saitoh, K. Ikeda, H. Kumada, *Intervirology* **2002**, *45*, 33.
[67] J. J. Feld, J. H. Hoofnagle, *Nature* **2005**, *436*, 967.
[68] R. Duncan, *Nat. Rev. Cancer* **2006**, *6*, 688.